

IMECE2007-41706

MECHANICAL/NAVAL DESIGN OF AN UNDERWATER REMOTELY OPERATED VEHICLE (ROV) FOR SURVEILLANCE AND INSPECTION OF PORT FACILITIES

Juan A. Ramírez

Universidad Pontificia Bolivariana
Department of Mechanical Engineering
P.O. Box 56006
Medellín, Colombia
telephone: 574-415-9020
fax: 574-411-8779
juan.ramirez@upb.edu.co

Rafael E. Vásquez*

Universidad Pontificia Bolivariana
Department of Mechanical Engineering
P.O. Box 56006
Medellín, Colombia
telephone: 574-415-9020
fax: 574-411-8779
rafavasquez@asme.org

Luis B. Gutiérrez

Universidad Pontificia Bolivariana
Department of Electrical and Electronics Engineering
P.O. Box 56006
Medellín, Colombia
telephone: 574-415-9020
fax: 574-411-8779
luis.gutierrez@upb.edu.co

Diego A. Flórez

Universidad Pontificia Bolivariana
Department of Mechanical Engineering
P.O. Box 56006
Medellín, Colombia
telephone: 574-415-9020
fax: 574-411-8779
diego.florez@upb.edu.co

ABSTRACT

This paper presents the mechanical/naval design process of an underwater remotely operated vehicle (ROV), required to obtain reliable visual information, used for surveillance and maintenance of ship shells and underwater structures of Colombian port facilities. The design was divided into four main subsystems: mechanical/naval, hardware, software and guidance, navigation and control. The most relevant design constraints were evaluated considering environmental conditions, dimensional restrictions, hydrostatics, hydrodynamics, degrees of freedom and the availability of instrumentation and control hardware. The mechanical/naval design was performed through an iterative process by using computational tools, including Computer Aided Design CAD, Computer Aided Engineering CAE, Computational Fluid Dynamics CFD and a high level

programming environment. The obtained design ensures that the reliable operation of the robot will be achieved by using a consistent construction process. The new ROV constitutes an innovative product in Colombia, and it will be used for surveillance and oceanographic research tasks.

Keywords: ROV, UUV, Underwater surveillance, Underwater maintenance, Mechanical design.

INTRODUCTION

Because of the 9/11 attacks in the United States, a general concern has appeared in the world to enhance the maritime security. According with this purpose, the International Maritime Organization stated new policies with respect to security in The International Ship and Port Facility Security Code (ISPS Code) [1].

*Address all correspondence to this author.

Due to the fact that the 95% of the world trade is made through maritime ways [2], it is necessary the implementation of an underwater inspection system to get reliable visual information of ship shells and underwater structures, in order to guarantee the appropriate security levels and the corresponding security measures in the trading ports of Colombia. The visual inspections include the identification of failures such as cracks, dents, deformations, incrustations and sedimentation among others.

There are different options to perform the inspections: Divers, Human Operated Vehicles (HOVs) and Unmanned Underwater Vehicles (UUVs) [3–5]. The most feasible and reliable alternative is the construction of an UUV which is denominated as a Remotely Operated Vehicle (ROV) which performs underwater inspections through a real-time video transmission of the underwater environment. The robot is operated from a surface station through a tether cable, reducing the danger for humans and the operational costs.

The ROVs have been used for surveillance and maintenance tasks in different fields such as: port industry, military industry, oceanographic research, acuaculture, marine biology, etc. This kind of vehicles could be classified in three main groups: heavy work, observation and micro/mini ROVs [6]. Although there are commercial prototypes of the three classes of ROVs, they are expensive and the purpose of the main project is the development of a low cost innovative product to perform underwater inspections in the Colombian ports of Cartagena, Santa Marta, Barranquilla and Buenaventura. The research group A+D (Automation and Design) from the Universidad Pontificia Bolivariana has developed two previous prototypes of ROV: VISOR I [7] and VISOR II [8,9], which represent an important experience in the development of unmanned underwater vehicles.

This paper addresses the design of a new ROV, required to bring reliable visual information, used for surveillance and maintenance of ship shells and underwater structures of Colombian port facilities.

CONCEPTUAL DESIGN

Conceptual design is the first design stage. Here the objectives are clearly defined, based on the review of the state-of-the-art and on the identification of the application's requirements. Hence, a list of design specifications must be obtained. Such specifications are required to start the basic design stage and they will be useful for making decisions.

Design methodology

The methodology used is based on a basic machine design process [10] and on the classic design spiral used in naval applications [3,11,12]. The design process is divided into three stages: conceptual design, basic design and detailed design. In the basic stage, the submersible is divided into subsystems and the design

spiral is used to iteratively decide the most appropriated solution for each of them. In the third stage, a synthesis/analysis process is used to define the form and the dimensions of each component of the vehicle and to define all the commercial elements.

Design constraints

The design constraints used in the design process are addressed below.

Environmental constraints The vehicle has to operate in the Colombian ports of Cartagena, Barranquilla, Santa Marta and Buenaventura. Therefore, parameters such as maximum depth, density, salinity, temperature and current velocity depends on a port/salt-water environment. Some water properties that must be considered are: low compressibility, high opacity to visible and radio electromagnetic radiation and transparency to acoustic wave transmission, among others [2].

Density, temperature and salinity. Water density depends on depth, temperature and salinity. In terms of temperature, it is known that water reaches its highest value around 4°C. In terms of salinity, the maximum possible density varies following Newman and Pierson equations, which show that density decreases when salinity increases. In terms of depth, salt water density varies from 1021 kg/m^3 at the surface to 1070 kg/m^3 at 1000 m depth [2]. In this application, salt water density is around 1024 kg/m^3 . Meadows and Meadows [2] state that water's temperature varies with depth, but in the range of 0 to 200 m, it could be considered constant and equal to the surface's temperature.

Electromagnetic radiation propagation. As depth increases, total radiation quantity decreases considerably. For practical purposes it could be said that for fresh water there is no visible light and is not possible to transmit radio waves from the surface to 100 m depth. This phenomenon is more severe in port salt water and turbid water. This particular constraint indicates that an illumination system and an umbilical cable are necessary components of the vehicle.

Working depth. The working depth defines the mechanical strength of all structural components, since the pressure applied by the liquid column above the vehicle could collapse it. Table 1 contains the maximum depth in the ports of Barranquilla, Buenaventura, Cartagena and Santa Marta. This suggests that maximum operational depth is about 18.3 m. A higher depth is chosen to avoid limitations to the operational capabilities of the vehicle. In this way, a 100 m maximum value is selected which is equivalent to a hydrostatic pressure of 1.00 MPa (145.5 psi).

Port	Maximum depth (m)
Barranquilla	12.0
Buenaventura	13.7
Cartagena	13.7
Santa Marta	18.3

Table 1. Colombian ports depth

Design depth. The design depth establishes a security margin for the collapse resistance of the hulls and other structural elements. This means that all structural calculations must be done at the design depth, in order to guarantee the integrity of the ROV at the working depth. In this case a depth of 165 m is chosen, which is equivalent to a hydrostatic pressure of 1.66 MPa (240 psi).

Vehicle weight and dimensions. It is desired that both weight and vehicle's dimensions be as smaller as possible. Since those variables are coupled, their ratio could be controlled to obtain a desired positive-neutral buoyancy. This could be done by making the vehicle's density slightly smaller than the density of the water. In addition, it is desired that the ROV system be easy to handle. Following these constraints, it has been defined that the vehicle's weight be less than 100 kg and it has to fit in a cubic box of 1 m side.

Hydrostatic and hydrodynamic considerations

A list of hydrostatic and hydrodynamic considerations is addressed by Allmendinger [3]. Such considerations include loads of interest, static equilibrium conditions, static and dynamic stability conditions and drag and thrust considerations:

Loads of interest. The loads that influence the behavior of the vehicle are:

- Weight.
- Displacement (force due to the gradient of pressure).
- Drag and lift (loads due to the relative motion between the vehicle and the water).
- Thrust.
- Contact forces (contacts with objects, waves, and wind).
- Inertial loads (due to vehicle changes in linear and angular momentum).

Static equilibrium. The buoyancy of a submersible is the algebraic difference between displacement and weight. The buoyancy of a submersible is positive when the displacement is greater than weight, negative when the displacement is less than weight and neutral when they are equal. As it was stated, it is desired that the vehicle's buoyancy be

positive-neutral, i.e. the difference between displacement and vehicle's weight must be small and positive.

Static stability. The static stability is guaranteed by locating the gravity center below the buoyancy center. This condition forces the submersible to recover its equilibrium position when it is angularly displaced about any axis located on the plane of motion.

Dynamical stability. This type of stability is also related to the location of the gravity and buoyancy centers. In this case the vehicle must have enough energy to recover its equilibrium position, which is guaranteed by separating the gravity center from the buoyancy center.

Drag and thrust. The thrust power must be able to overcome drag at operational speed, also during acceleration intervals.

Mobility The vehicle should be able to move in any direction and follow any trajectory: forward/backward (surge), ascent/descent (heave) and lateral displacement (sway). It is also required that it could be headed in any direction (yaw), i.e. rotational motion around a vertical axis. Such movements must be controlled by using the propulsion system.

Operational speed Since the ROV must keep an equilibrium position in spite of the disturbances because of currents. The operational speed depends on the highest port current speed. Accordingly to port's conditions, the maximum operational speed is defined as 1.5 m/s.

Instrumentation, control, power and communications devices Instrumentation, control, power and communication devices are needed to allow appropriate operational conditions for the vehicle. The instrumentation's weight and volume must be considered in the mechanical/naval design because of the buoyancy and dimensional constraints.

Control. A main on-board computer, whose principal tasks are to process instrument's measurements and to deliver control signals to the propulsion system, is required. It is used to perform low level stabilization tasks, i.e. it has to answer properly to operator's commands.

Measurement instruments. This application is fulfilled by the following instruments: an inertial measurement unit (IMU), a digital compass (Magnetometer), a depth meter and a thermometer.

Power. The ROV needs internal DC power sources, in order to supply energy to the actuators and the instruments. In addition, drivers and power amplifiers for the actuators are also needed.

Communication. Communications between the ROV and the surface station require fiber optic and transceiver devices.

Design specifications

The final design specifications are shown in table 2.

Characteristic	Value
Vehicle type	Observation range
Environment	Port salt-water
Density	1024 kg/m ³
Operation depth	100 m
Design depth	165 m
Temperature range	0–40°C
Mobility	Four degree-of-freedom: surge, sway, heave, yaw
Speed	1.5 m/s
Buoyancy	neutral/positive
Maximum weight	100 kg
Communications technology	Fiber optic
Navigation instruments	IMU, depth meter and digital compass
Auxiliary systems	Illumination and communication Instruments for analysis

Table 2. Design specifications

BASIC DESIGN

The ROV system is divided into three main subsystems: the surface station, the submersible and the communication system between them (figure 1). The surface station contains operator’s control devices such as: surface computer with man/machine interface, a joystick used to control vehicle’s movement and an electric power plant. The communication system is composed of



Figure 1. Vehicle's subsystems

an umbilical cable which is made up of four fiber optics and AC power conductors.

Subsystems of the vehicle

The vehicle is divided on four subsystems: the structure, the propulsion system, the electric/electronic devices and the illumination system.

Structure A single cylindrical hull with two hemispheric ends is used to keep all ROV components. This cylindrical hull is protected with an external frame. At least one of the hemispheric ends must be translucent.

Propulsion system A four-screwed-propeller-thruster system is used. Two of them are used to provide *surge* displacement and *yaw* rotation. One thruster is used to provide *heave* displacement, and the last one is used to provide *sway* displacement, Figure 2. The following considerations are taken:

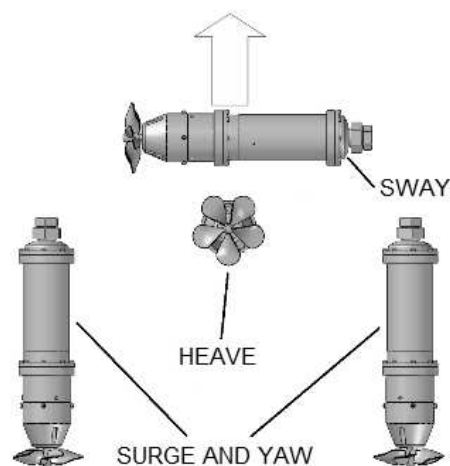


Figure 2. Thruster configuration. The arrow shows the forward direction.

- The line of action of the heave direction thruster has to cross the center of mass, in order to avoid roll and pitch movements.

- The surge/yaw thrusters have to be parallel and their line of action have to be vertical at the same height of the center of mass in order to avoid pitch movements.
- The sway direction thruster has to be in the same height as the surge/yaw case. Since it is impossible that this thruster's line of action crosses the center of mass, it generates an undesired yaw movement which has to be compensated by the surge/yaw thrusters.

Each thruster has a brushless DC motor in a cylindrical hull, a dynamic sealing system and a screw propeller. To select an electric DC brushless motor, the following criteria were considered:

- AC electric motors are mostly used in high power applications (i.e. 1/3 hp or higher). Additionally this kind of motors are usually intended for industrial applications, so their design and shape are not compact.
- Brushed electric motors exhibit wear problems which require attention and maintenance, Such kind of problems are avoided using the brushless ones.
- Starting currents are usually higher in brushed electric motors, compared with brushless ones.

The sealing system used is made up with a mechanical seal which has two pieces a stationary and a rotary part, with a tungsten-carbide mirror-finished-surface interface which prevents leaking. The sealing's configuration is shown in figure 3.

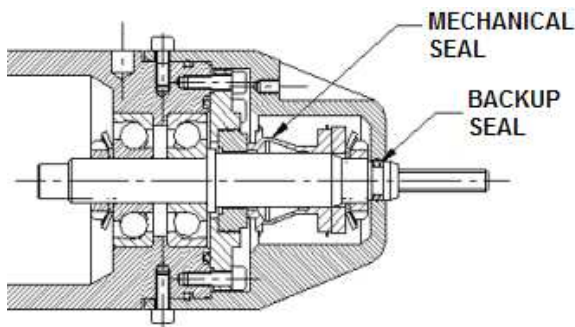


Figure 3. Mechanical seal

Electronic devices All electronic devices are connected to the chosen measurement instruments, power electronics, control and communications. The hardware architecture used is shown in figure 5.

On-board video camera. A SONY SNC50 surveillance IP video camera with zoom, pan and tilt capabilities is selected. This kind of camera facilitates the video transmission process without using any extra software.

Power electronics. Each brushless DC motor uses an amplifier driver able to control speed in open or closed loop. Additionally, two AC/DC power supply are selected: the first one for the propulsion system, with 600 W power and the second one for the instruments, with 200 W power.

Navigation instruments. A 0–13.7 bar (0–200 psi) range depth meter is selected. Also a MEMS-based inertial measurement unit is selected, which is provided with gyroscopes, accelerometers and a digital compass.

Additional measurement instruments. A platinum resistance temperature detector (RTD Pt100) with a 4–20 mA output transmitter is selected to measure environment temperature.

On-board computer. A PC104 embedded processor with a real-time operating system (RTLinux™) is selected.

Communication devices. A fiber optic/ethernet transceiver is required in both umbilical cable ends, and an ethernet switch is required to keep both camera and processor in the same network. Internally a CAN bus is used to integrate all measurement instruments and actuator command information on the same network.

Illumination system The illumination system is made up of four single halogenous lights, mounted in the front part of the protecting frame. Each light bulb is protected by a cylindrical hull. The light configuration is shown in figure 4.

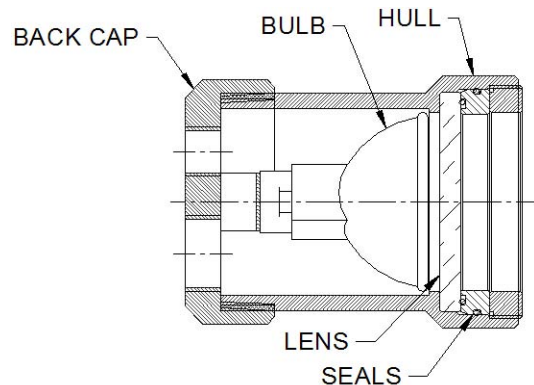


Figure 4. Light configuration

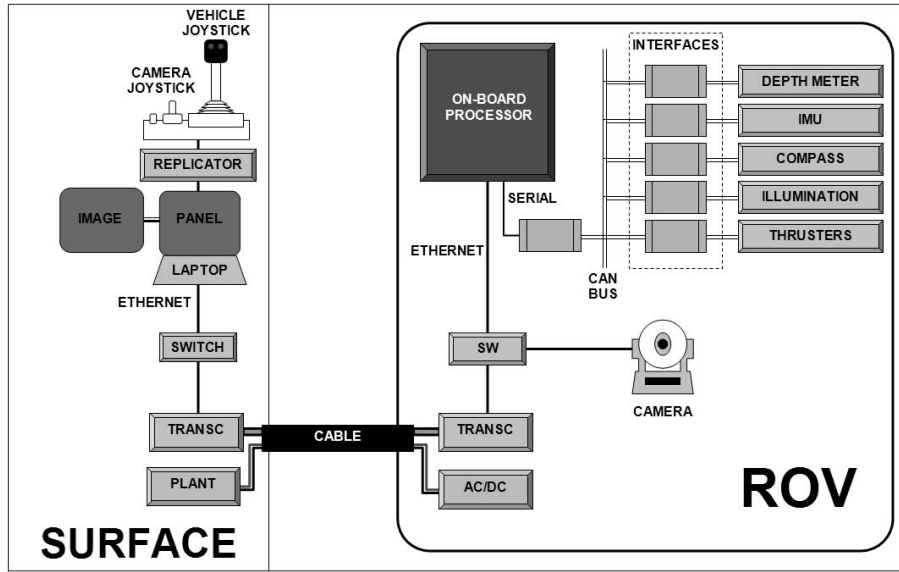


Figure 5. Hardware architecture

Subsystems integration

All subsystems integrated on a basic 3D sketch is shown in figure 6.

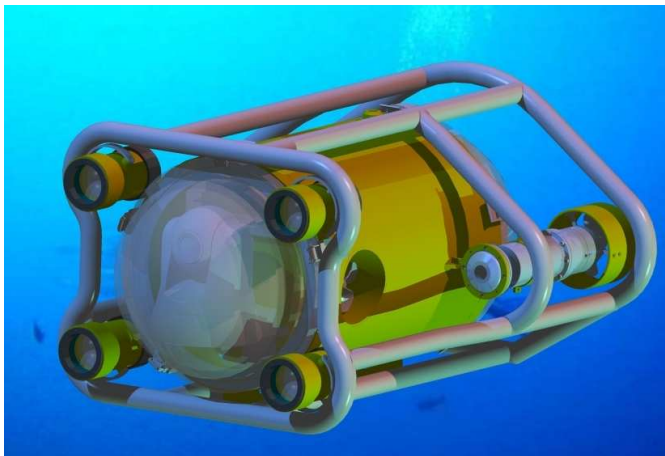


Figure 6. Vehicle basic design

DETAILED DESIGN

In this section some of the calculations required to guarantee vehicle components functionality are presented. As expected, the main results of this stage are the detailed drawings required for manufacturing.

Hull

As it was stated, the hull of the submersible is made up with two kinds of shells, a cylindrical aluminum shell and two hemispherical acrylic shells. For each one of these components, an structural analysis must be performed.

Cylindrical shell A first collapse resistance calculation is made using the collapse pressure equation for a cylindrical hull addressed by Nash [13].

$$p = \frac{2.42E}{(1 - \mu^2)^{\frac{3}{4}}} \left[\frac{\left(\frac{h}{2R}\right)^{\frac{5}{2}}}{\frac{L}{2R} - 0.45 \left(\frac{h}{2R}\right)^{\frac{1}{2}}} \right] \quad (1)$$

Where p is the collapse pressure, h is the hull thickness, L is the cylinder length, R is the cylinder mid surface radius, E is the Young's modulus and μ is the Poisson's ratio. The data and results are shown in Table 3. More exact calculations were made by using a finite elements analysis (FEA) software (UnigraphicsNX™) in which the exact hull geometry was considered. Some results are shown in Table 4 and in Figure 7.

Hemispherical shells An initial calculation was made by using the collapse pressure equation addressed by Nash [13]:

$$p = \frac{2Eh^2}{R^2 \sqrt{3(1 - \mu^2)}} \quad (2)$$

Property	Magnitude
E	68.9 GPa
μ	0.33
R	163.4 mm
L	384 mm
h	4 mm
p	2.68 MPa (388.4 psi)

Table 3. Hull cylinder data and results

S_y (yield strength)	276 MPa
Maximum Von Mises stress	203 MPa
Maximum displacement	0.796 mm
Static security margin	1.18

Table 4. Hull cylinder finite element simulation

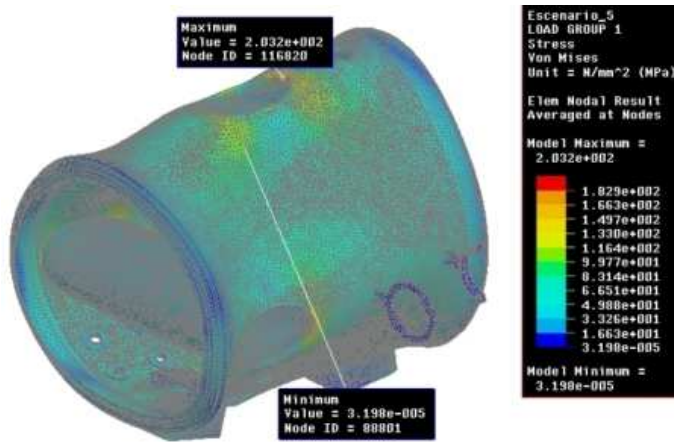


Figure 7. Hull FEA

Property/Result	Magnitude
E	2.2 GPa
μ	0.33
R	145 mm
h	7 mm
p	6.27 MPa (1856.4 psi)

Table 5. Hull hemisphere data and results

S_y (yield strength)	48 MPa
Maximum Von Mises stress	22.57 MPa
Maximum displacement	1.032 mm
Static security margin	2.13

Table 6. Hull cylinder finite element simulation

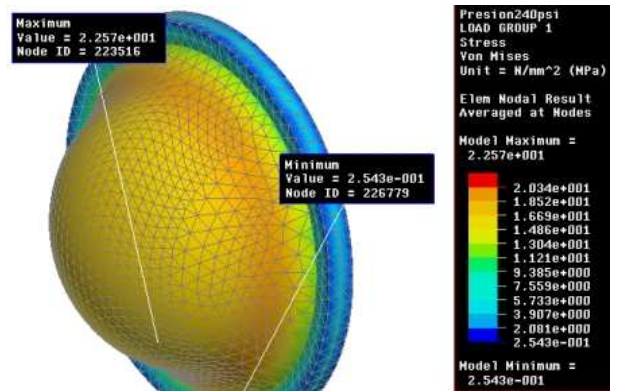


Figure 8. Dome FEA

considerations:

$$\int_0^{\Delta_{\max}} E dx - \int_0^{\Delta_{\max}} F(x) dx = -\frac{1}{2}mv^2 \quad (3)$$

Where $F(x)$ is a function that relates the force acting in the center of the shell with the maximum deformation, Δ_{\max} is the maximum deformation when the speed of the vehicle reaches zero value, E is the total thrust, m is the weight and v is the speed of the vehicle before the crash. $F(x)$ is a linear function obtained through FEA simulations:

$$F(x) = \left(50798 \frac{\text{N}}{\text{mm}}\right) x \quad (4)$$

Where particularly R is the mid surface radius of the hemisphere, the other parameters have the same meaning as before. Data and results are shown in Table 5. Again, better calculations were made by using FEA and using the exact geometry. Some results are shown in Table 6 and in Figure 8. Additionally, an impact analysis is required to design the hemispheric shell. The work and energy principle is used considering that the vehicle crashes at 1.5 m/s against a rigid static wall under the influence of the thruster action. This means that all ROV kinetic energy is converted in strain energy under the action of thrust. Under this

Equations (3) and (4) yield:

$$50798\Delta_{\max}^2 - E\Delta_{\max} - \frac{1}{2}mv^2 = 0 \quad (5)$$

It is also possible to obtain a relationship between maximum deformation and maximum Von Mises stress:

$$\sigma(x) = \left(14.051 \frac{\text{MPa}}{\text{mm}}\right)x \quad (6)$$

If it is assumed that for the vehicle $m = 60$ kg, $v = 1.5$ m/s, $E = 58$ N, solving (5) and (6) yield $\sigma(\Delta_{\max}) = 16.2$ MPa.

Propulsion

The design of this subsystem includes the evaluation of the drag forces and the required power. It is also required to calculate the mechanical resistance of structural components.

Drag forces The calculation of drag forces as a function of speed is achieved through simulation by using Computational Fluid Dynamics (CFD) software (CosmosflowTM) (Figure 9). The results are shown in Figure 10 where F_{Ai} is the drag force

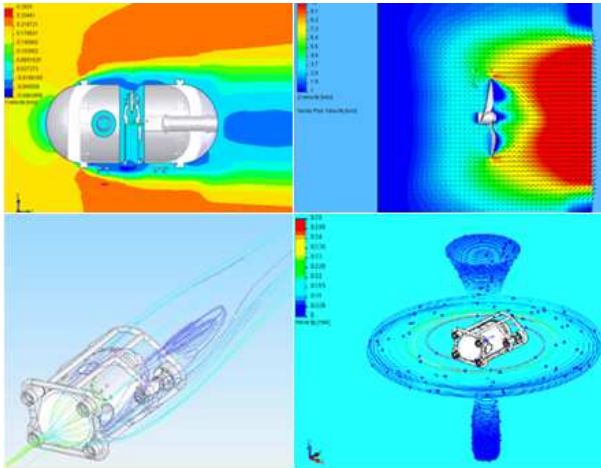


Figure 9. CFD analysis

in the direction i , considering that surge is x direction, sway is y direction and z is heave direction.

Thrust Thrust is calculated as a function of drag force using the equation [14]:

$$T = \frac{F_A}{1-t} \quad (7)$$

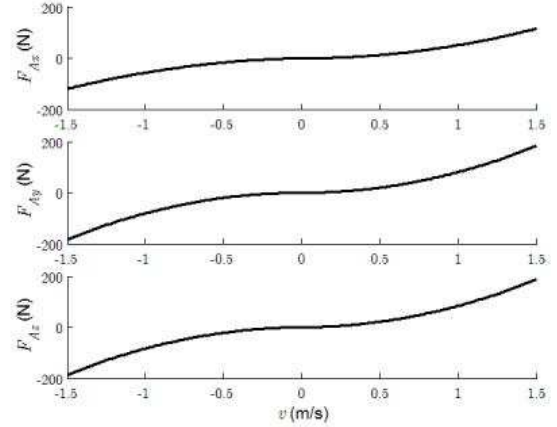


Figure 10. Drag forces

where T is the thrust, F_A is the drag force and t is a quantity known as thrust deduction, which is assumed to be zero because drag calculations include the effects of all vehicle components. The drag force is assumed to have the following form

$$F_A = K_{A1}v + K_{A2}v|v| \quad (8)$$

where K_{Ai} are constant parameters. On the other hand, the thrust force T and propeller shaft torque Q , according to the momentum theory [14], have the following form:

$$T = K_T \rho D^4 \omega |\omega| \quad (9)$$

$$Q = K_Q \rho D^5 \omega |\omega| \quad (10)$$

where K_T is a parameter known as thrust coefficient, K_Q is the torque coefficient, D is the diameter of the propeller and ω is the angular velocity. The thrust and torque coefficients are a function of an advance coefficient ($K_T = K_T(J)$ and $K_Q = K_Q(J)$), defined as:

$$J = \frac{v_A}{\omega D} \quad (11)$$

where v_A is the speed of advance which is defined as a function of the speed of the vehicle v and a quantity known as wake fraction w , which is assumed to be zero as a first guess.

$$v_A = v(1-w) \quad (12)$$

The relationship between K_T , K_Q and J is usually obtained through tests. So, for a first approach Wageningen B series propeller curves were used. This application uses a 3.5" propeller

with a 4" pitch and a blade area ratio (A_E/A_0) of 0.70. Substituting (8) and (9) into (7):

$$2K_T \left(\frac{v}{\omega D} \right) \cdot \rho D^4 \omega |\omega| - K_{A1} v - K_{A2} v |v| = 0 \quad (13)$$

The numerical solution of (10) and (13) is shown in the figure 11. From these results it is clear that the maximum torque is 864 mNm.

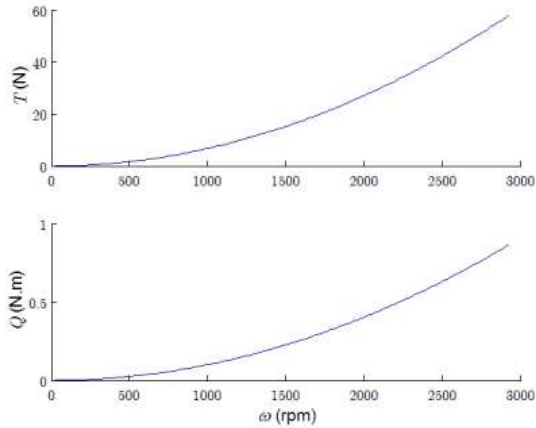


Figure 11. Torque and thrust

Thruster hull resistance Hull resistance is calculated through FEA simulation and some of the results are shown on Table 7. As it could be noticed, the mechanical resistance of this particular part is considerably high, because its dimensions are constrained by manufacturing capabilities and functional requirements, and not only by the collapse resistance.

S_y (yield strength)	215 MPa
Maximum Von Mises stress	20.2 MPa
Maximum displacement	0.006 mm
Static security margin	10.6

Table 7. Thruster finite element simulation results

Illumination

The mechanical resistance of the light hull must be calculated when it is submerged at the design pressure, i.e. hydrostatic pressure of 16.5 bar (240 psi). Because of the geometry,

calculations were achieved through FEA simulation. Some of the results are shown in Table 8.

S_y (yield strength)	215 MPa
Maximum Von Mises stress	33 MPa
Maximum displacement	0.007 mm
Static security margin	6.52

Table 8. Light finite element simulation results

Design integration

Detailed design integration requires that static and dynamic stability are guaranteed, and the verification of buoyancy conditions.

The first step is to calculate the buoyancy center and the displacement when all components are integrated. It allows a strategic addition of masses that assure the desired stability conditions. The first calculations are shown in table 9.

The same procedure is used for static and dynamic stability conditions. In this case is possible to evaluate them through the mass properties calculation. The initial values are shown in table 10.

Displacement	56.74 kg
Buoyancy center x	-3.21 mm
Buoyancy center y	0.66 mm
Buoyancy center z	1.49 mm

Table 9. Buoyancy initial conditions

Weight	51.67 kg
Mass center x	5.40 mm
Mass center y	1.19 mm
Mass center z	16.21 mm
Inertia product xy	0.010810 kg m ²
Inertia product xz	-0.004656 kg m ²
Inertia product yz	-0.003811 kg m ²

Table 10. Stability initial conditions

The next step is to distribute the internal components and to add dead masses which guarantee that vertical distance (z direction) between mass center and buoyancy center is 25 mm, with the mass center placed below the buoyancy center. Distance in x and y directions must be approximately zero. It could be concluded from tables 9 and 10 that there is a wide margin between weight and displacement which shall be used to balance buoyancy and stability by adding dead masses.

CONCLUSIONS

The design of the submersible vehicle was developed following a process of three stages: conceptual, basic and detailed design. In the first stage the specifications of the vehicle were obtained in concordance with the application's necessities and the state-of-the-art. In the second stage a functional subsystem division was made, and for each subsystem a basic configuration was defined to fit desired specifications. In the third stage all subsystems' qualities were defined through engineering calculations and simulation using specialized software.

In the conceptual design stage, a list of specifications was made for the underwater remotely operated vehicle, by taking in account its operational conditions.

The basic design allows one to have a clear idea of how the vehicle is going to be after it be manufactured. It includes knowledge of the components distribution and technical features of each subsystem to make the vehicle functional.

The detailed design was performed through structural and operational calculations based on analytical and computational mechanics of materials, computational fluid dynamics and classical rigid body mechanics. An appropriate design will guarantee component reliability related to mechanical resistance and functionality.

The design of the vehicle presented here, is a first approach aiming at a refined and definitive design. As it was stated, some developments require laboratory tests related to propulsion system performance and vehicle drag forces, which suggest that a final design might present differences with the actual one.

ACKNOWLEDGEMENTS

This project is developed with the founding of the Colombian Institute for the Development of Science and Technology *Francisco José de Caldas COLCIENCIAS*, the Universidad Pontificia Bolivariana and the Escuela Naval Almirante Padilla. Code 121014-17909, contract # 300 of 2005.

REFERENCES

- [1] International Maritime Organization, 2002. The International Ship and Port Facility Security Code (ISPS Code) .
- [2] Meadows, G. and Meadows, L., 2003. *Ship design and construction*, Vol. 1. The society of naval architects and marine engineers, Jersey City (NJ), ch. The marine environment, pp. 1 – 16.
- [3] Allmendinger, E., 1990. *Submersible vehicle systems design*. The society of naval architects and marine engineers, Jersey City (NJ).
- [4] Griffiths, G., 2003. *Technology and applications of autonomous underwater vehicles*. Taylor & Francis, London.
- [5] Ross, C., 2006. "A conceptual design of an underwater vehicle". *Ocean Engineering*, **33**, pp. 2087–2104.
- [6] ROVEXCHANGE, 2006. Rov specifications & reviews. [online] <http://www.rovexchange.com>.
- [7] Cadavid, R. et al., 1995. VISOR: Vehículo para investigación subacuática operado remotamente. Tesis Ingeniería Mecánica, UPB, Medellín.
- [8] Correa, J. et al., 1998. "Consideraciones de diseño para un vehículo subacuático controlado en forma dual: autónomamente y vía cable". In *Memorias del VII Congreso Latinoamericano de Control Automático*, ACCA.
- [9] García, D., and Sarria, C., 1999. Diseño y construcción de la carcasa estructural de un ROV. Tesis Ingeniería Mecánica, UPB, Medellín.
- [10] Norton, R., 2005. *Machine Design: An Integrated Approach*, 3rd ed. Prentice Hall, New Jersey.
- [11] Lamb, T., 2003. *Ship design and construction*, Vol. 1. The society of naval architects and marine engineers, Jersey City (NJ).
- [12] Gale, P., 2003. *Ship design and construction*, Vol. 1. The society of naval architects and marine engineers, Jersey City (NJ), ch. The ship design process, pp. 1 – 39.
- [13] Nash, J., 1995. *Hydrostatically loaded structures*. Pergamon, New York.
- [14] Allmendinger, E. et al., 1990. *Submersible vehicle systems design*. The society of naval architects and marine engineers, Jersey City (NJ), ch. Hydromechanical principles, pp. 191–269.